J. Biochem. **144,** 371–381 (2008)
doi:10.1093/jb/mvn077

Agonistic and Antagonistic Effects of C5a-Chimera Bearing S19 Ribosomal Protein Tail Portion on the C5a Receptor of Monocytes and Neutrophils, Respectively

Yuuichiro Oda[1,2], Kazutaka Tokita[1], Yoshihiko Ota[1], Ying Li[1], Keisuke Taniguchi[1,3], Norikazu Nishino[4], Katsumasa Takagi[2], Tetsuro Yamamoto[1] and Hiroshi Nishiura[1,*]

[1]Department of Molecular Pathology; [2]Department of Orthopedic and Neuro-Musculoskeletal Surgery, Faculty of Medical and Pharmaceutical Sciences, Kumamoto University; [3]Division of Pharmacology, Kumamoto Laboratory, Mitsubishi Chemical Safety Institute of Laboratory, Kumamoto; and [4]Department of Biological Functions and Engineering, Graduate School of Life Science and Systems Engineering, Kyushu Institute of Technology, Kitakyushu, Japan

Received May 11, 2008; accepted May 24, 2008; published online May 31, 2008

C-terminus of S19 ribosomal protein (RP S19) endows the cross-linked homodimer with a dual effect on the C5a receptor in leucocyte chemoattraction; agonistic effect on the monocyte receptor, and antagonistic effect on the neutrophil receptor. C5a exhibits the uniform agonistic effect on this receptor of both cell types. We have currently prepared a recombinant C5a-chimeric protein bearing the C-terminus of RP S19 (C5a/RP S19 chimera) to be used as a substitute of the RP S19 dimer. *In vitro*, this chimera similarly inhibited the intracellular Ca^{2+} mobilization of neutrophils induced by C5a to the RP S19 dimer did. In the guinea pig skin, 10^{-7}M C5a/RP S19 chimera exhibited an inhibitory capacity to the neutrophil infiltration induced by 3×10^{-7}M C5a without enhancing monocyte infiltration. In reverse passive Arthus reaction, the neutrophil infiltration associated with plasma extravasation was significantly reduced by the simultaneous administration of 10^{-7}M C5a/RP S19 chimera with antibodies. The C5a/RP S19 chimera is a useful tool not only to examine the molecular mechanism that underlies the functional difference of the C5a receptor between monocytes and neutrophils, but also to prevent C5a-mediated hyper-response of neutrophils in acute inflammation.

Key words: C5a, C5a receptor, monocytes, neutrophils, S19 ribosomal protein.

Abbreviations: BSA, bovine serum albumin; C5a/RP S19 chimera, recombinant C5a-chimeric protein bearing the C-terminus of RP S19; FBS, fetal bovine serum; fMLP, formyl-Met-Leu-Phe; HBSS, Hanks' balanced salt solution; HPLC, high performance liquid column chromatography; OVA, ovalbumin; PAGE, polyacrylamide gel electrophoresis; RP S19, ribosomal protein S19; SDS, sodium dodecyl sulphate.

The ribosomal protein S19 (RP S19) dimer was first isolated from the rheumatoid arthritis synovial lesion as the major monocyte/macrophage chemotactic factor (*1*). Later, it was also detected in atherosclerotic lesion of the aorta (*2*). The RP S19 dimer is formed by a transglutaminase-catalysed reaction and released from cells during apoptosis (*3–5*). Dimerization endows RP S19 with a ligand function at the chemotactic C5a receptor. It is well known that the C5a receptor was initially identified as the receptor of C5a, the complement C5-dericed leucocyte chemotactic factor. Different from C5a, the RP S19 dimer exhibits an agonistic and antagonistic dual effect on monocytes and on neutrophils, respectively, resulting in monocyte-predominant infiltration (*6*). The monocyte infiltration induced by the RP S19 dimer released from apoptotic cells *in vivo* results in the phagocytic clearance of these apoptotic cells without macroscopic inflammatory signs (*4*). Consistently, the RP S19 dimer induced the respiratory burst reaction of monocytes, and inhibited the same reaction of neutrophils induced by C5a (*7*).

We have identified sub-molecular regions of RP S19 that are responsible for two-step binding to the monocyte C5a receptor and for the antagonist to the neutrophil C5a receptor (*8*, *9*). Following the dimerization, a basic cluster of RP S19 formed by tandem basic amino acid residues becomes capable of interacting the N-terminal region of the C5a receptor similar to the three-dimensional arrangement of basic residues in C5a. The regions of the RP S19 dimer and C5a that involve in the second binding step are –Leu131–Asp132–Arg133– and –Leu72–Gly73–Arg74–COOH, respectively, where the β-carboxyl group of Asp132 of the former functions equivalently to the α-carboxyl group of Arg74 at the C-terminus of C5a (*8*). Even though the over-all homology in the primary structure between C5a and RP S19 is only 4% (*6*), the amino acid sequences at their second binding sites that activate the C5a receptor resemble.

The key region of RP S19 involved in the switch between agonistic and antagonistic effects on the C5a receptor of neutrophils is from Ile134 to Lys144, which is absent in the C5a molecule (*9*). The C5a receptor gene is

*To whom correspondence should be addressed.
Tel: 81963735306, Fax: 81963735308,
E-mail: seino@kumamoto-u.ac.jp

a single gene (*10*), and we have read no report on alternative splicing of the C5a receptor gene product, while the functional difference in response to the RP S19 dimer is obvious between the neutrophil receptor and the monocyte one. The above information suggests that the presence or absence of an interaction with the C-terminal region of RP S19 would determine the functional subtype of the C5a receptor between the neutrophil and the monocyte.

We propose that the RP S19 dimer is a good experimental tool to induce monocyte-predominant leucocyte infiltration *in vivo* or to distinguish between the functional sub-types of C5a receptor expressed on different cell types. Conceivably, the RP S19 dimer could also be a therapeutic tool to inhibit the C5a-mediated neutrophil infiltration. However, it is not easy to prepare a large quantity of the RP S19 dimer; dimerization using transglutaminases *in vitro* results in >80% of inactive RP S19 with an intra-molecular cross-link and only <20% of the active RP S19 dimer with the inter-molecular cross-link. Alternatively, we have synthesized a 22 amino acid residue peptide with the sequence of the C-terminus of C5a with the Gly73Asp substitution and the sequence of the switching moiety of RP S19. Although the small chimeric peptide reproduced the function of the RP S19 dimer *in vitro*, it was not useful *in vivo* because of the absence of the glycosaminoglycan-binding moiety of RP S19 (Lys23–Lys29) responsible for molecular retention at interstitial tissue (*9*). An intradermal injection of this chimeric peptide into experimental animals failed to induce the monocyte infiltration (Nishiura et al., unpublished observation).

To overcome these problems, we have currently prepared a recombinant chimeric protein (C5a/RP S19 chimera) possessing the full body of C5a and the C-terminal switching region of RP S19 with a substitution of Gly73 of C5a by Asp. We have investigated in the guinea pig skin whether C5a/RP S19 chimera would induce the monocyte-predominant infiltration and whether C5a/RP S19 chimera would inhibit the neutrophil infiltration induced by C5a. These results are expected if the C5a/RP S19 chimera should be a useful tool, as a substitute of the RP S19 dimer for *in vivo* experiments.

In our previous studies, we have demonstrated that the guinea pig is a useful experimental animal to analyse the RP S19 dimer-related phenomena: the amino acid sequence of RP S19 is identical between the human and the guinea pig, and monocytes and neutrophils of the guinea pig respond to the RP S19 dimer in a similar manner to those of the human, although higher concentration of the molecule is needed to attract guinea pig leucocytes as observed in the case of formyl-Met-Leu-Phe (fMLP) (*11*). Furthermore, different from the mouse C5a receptor, the guinea pig C5a receptor accepted human C5a as an agonistic ligand. These are reasons why we have used guinea pigs in the current study.

MATERIALS AND METHODS

Animals—Albino–Hartley strain male guinea pigs (400–550 g body weight), which were specific pathogen free, were purchased from Kyudo Corp. (Kumamoto, Japan). They were maintained in the Center for Animal Resources and Development, Kumamoto University. The animal experiments were performed under the control of the Ethical Committee for Animal Experiment, Kumamoto University School of Medicine.

Reagents and Others—RPMI 1,640 medium and Hanks' balanced salt solution (HBSS) were purchased from Nissui Pharm. Co. (Tokyo, Japan). Fura2-AM and HEPES buffer were products of Dojindo Laboratories Co. (Kumamoto, Japan). Fetal bovine serum (FBS) was a product of GIBCO BRC (Paisley, Scotland). Ficoll-Paque Plus®, columns for high performance liquid column chromatography (HPLC) such as Hi-Trap™ Chelating HP, Hi-Trap™ Heparin HP and Hi-Trap™ Benzamidine FF (high sub) and ECL Plus Western Blotting Detection System were obtained from Amersham Biosciences KK (Tokyo, Japan). Bovine serum albumin (BSA), ovalbumin (OVA) and fMLP were purchased from Sigma Chemical (St Louis, MI). A multi-well chamber for chemotaxis assay was a product of Neuro Probe (Bethesda, MD). Nucleopore filters were purchased from Nucleopore (Pleasant, CA). pET32a vector and Rosseta gami(B) Lys-S *Escherichia coli* strain were purchased from Novagen (Darmstadt, Germany). pBS(+)13 vector and JM109 *E. coli* strain were obtained from Stratagene (San Diego, CA). The restriction enzymes used were purchased from TaKaRa Biomedicals (Otsu, Japan). Immobilor Transfer Membrane™ was a product of Millipore (Billerica, MA). Anti-OVA rabbit IgG were a product of Polysciences, Inc. (Warrington, PA). An anti-C5a rabbit antiserum was a product of Calbiochem (La Jolla, CA). Horseradish peroxidase (HRP)-conjugated anti-rabbit IgG goat IgG were products of Santa Cruz Biotechnology (Santa Cruz, CA). Block Ace™ was purchased from Dainippon Pharmaceutical (Suita, Japan). OptiPrep™ was a product of AXIS-SHIELD PoC AS (Oslo, Norway). All other chemicals were obtained from Nacalai Tesque (Kyoto, Japan) or from Wako Pure Chemicals (Osaka, Japan) unless otherwise specified. The C5a receptor antagonistic/partial agonistic peptide, NMePhe-Lys-Pro-dCha-dCha-dArg, was synthesized as described previously (*12*). This peptide competitively inhibits the interaction of C5a to the second binding site of C5a receptor up to 10^{-6} M. Anti-RP S19 rabbit IgG and a rabbit antiserum against the synthetic C-terminal peptide of RP S19 (Arg-Lys-Leu-Thr-Pro-Gln-Gly-Gln-Arg-Asp-Leu-Asp-Arg-Ile) were prepared as described previously (*13*).

Preparation of C5a/C5a/RP S19 Chimera—The recombinant proteins were prepared using an *E. coli* expression system with pET32a vector and Rosseta gami(B) Lys-S as the host bacteria. Because the recombinant proteins should correctly form three intramolecular disulphide bonds, the recombinant precursor proteins were designed with Trx-tag before His-tag and S-tag at their N-terminal portions, and the initial two tags were finally removed by limited proteolysis with thrombin. The wild type human C5a has the six highly conserved cysteine residues, and a non-conserved Cys27 that does not involve the disulphide bridges. We therefore substituted Cys27 by Arg (C27R-C5a) according to the report of Paczkowski *et al*. (*14*).

In C5a/RPS19 chimera Gly73 of C5a was substituted with Asp (C27R-G73D-C5a) to compensate for the lost

Table 1. **List of the synthesized primer oligonucleotides.**

C5a-s	5′CGCGGATCCACACAGGAAACAGCTATG3′
C5a-as	5′CGGAATTCCGCTAACGACCCAGTTGCAT3′
C5a/RPS19-as1	5′AGCTGCCACCTGTCCGGCGATT CTGTCC AGTTGCATGTCTTTGTG3′
C5a/RPS19-as2	5′CGGAATTCCGCTAATGCTTCTTGTTGGC AGCTGCCACCTGTCC3′

's' and 'as' mean sense and anti-sense primers. Overlapped sequences are underlined.

α-carboxyl group of Arg74 (used for peptide bond formation in the chimera) by the β-carboxyl group of Asp73. This compensation is required in the binding to C5a receptor as described above.

We initially prepared C27R-C5a and C27R-G73D-C5a/RP S19 chimera cDNAs by the polymerase chain reaction (PCR). The primers used are listed in Table 1. The template used for the C27R-C5a cDNA preparation was pQE-30/C27R-C5a that had been kindly provided by Dr P. Monk of University Sheffield, UK. The primers used were C5a-s and C5a-as. PCR condition to prepare C5a cDNA was 94°C for 20 s, 60°C for 20 s and 72°C for 30 s, for denature, annealing and elongation, respectively, for 40 cycles. In the case of C27R-G73D-C5a/RP S19 chimera cDNA preparation, we used the nested PCR method. In the initial PCR, we used pQE-30/C27R-C5a as the template, and C5a-s and C5a/RPS19-as1 as the sense and antisense primers, respectively. The condition of this PCR was 94°C for 30 s, 57°C for 30 s and 72°C for 60 s, for the denature, annealing and elongation, respectively. We cut the PCR product with BamH1 and T4 polymerase, and inserted into pBS(+)13 cut with BamH1 and EcoRV. After confirming the nucleotide sequence, we used the recombinant pBS(+)13 as the template, and C5a-s and C5a/RPS19-as2 as the sense and antisense primers, respectively. In the second PCR, the PCR condition was the same as the initial PCR. By the second PCR, we obtained the C5a/RP S19 chimera cDNA. We inserted each cDNA thus prepared into pBS(+)13 cloning vector between BamH1 and EcoR1 restriction sites to confirm the nucleotide sequence. Since the sequences were correct, we respectively inserted the cDNAs into pET32a vector between BamH1 and EcoR1 sites.

Expression host *E. coli*, Roestta-gami(B) Lys-S, were transformed with one of the cDNA bearing pET32a. The transformed cells were cultured in NZYCM medium containing ampicillin, chloramphenicol, kanamycin and tetracycline at 37°C with continuous shaking. When the absorbance at 600 nm of the bacterial suspension became 0.6, the suspension was added with isopropyl 1-thio-β-D-galactoside at a final concentration of 1 mM, and incubated for another 5 h.

The cultured *E. coli* cells were recovered by centrifugation at 6000*g* for 10 min at 4°C, and resuspended into 1/10 culture volume of 20 mM Tris–HCl containing 200 mM NaCl and 10 mM EDTA (pH 8.0). The bacterial cell wall was broken by sonication in the presence of 1% Triton X-100, followed by centrifugation at 20,000*g* for 20 min at 4°C.

The supernatant was dialysed against 20 mM Tris–HCl buffer containing 500 mM NaCl and 5 mM imidazole (pH 8.0) at 4°C overnight, and applied to the Hi-Trap™ Chelating HP column pre-loaded with 1 ml of 100 mM $NiSO_4$. After washing the column with the dialysis buffer, the bound molecules were eluted with the same buffer except for containing 500 mM imidazole (pH 8.0). The eluate was dialysed against 20 mM Tris–HCl containing 30 mM NaCl (pH 7.5) for 4 h at 4°C, and applied to the Hi-Trap™ Heparin HP column equilibrated with the dialysis buffer. After washing with the same buffer, the bound molecules were eluted with the same buffer except for containing 1 M NaCl. The eluate was composed of a single molecule, Trx-tag-His-tag-S-tag-C5a or Trx-tag-His-tag-S-tag-C5a/RP S19 chimera.

The buffer was changed to 50 mM Tris–HCl buffer containing 50 mM NaCl and 10 mM $CaCl_2$ (pH 8.0) by dialysis at 4°C overnight, then the recombinant proteins were treated with thrombin at a ratio of 25 μg recombinant protein/unit thrombin for 1 h at 37°C to cut off the Trx-tag-His-tag portion. The reaction mixture was then applied to the Hi-Trap™ Benzamidine FF (high sub) column equilibrated with 50 mM Tris–HCl buffer containing 50 mM NaCl (pH 8.0) to remove thrombin. S-tag-C5a and S-tag-C5a/RP S19 chimera were finally separated by re-chromatography with the Hi-Trap™ Heparin HP column in the same condition as described above.

Western Blotting Analysis—Polyacrylamide gel electrophoresis (PAGE) was performed on a vertical slab gel of 20% polyacrylamide according to the method of Laemmli (*15*). The sample was boiled for 2 min in the presence of sodium dodecyl sulphate (SDS) and β-mercaptoethanol, and then applied to the gel. After electrophoresis at 20 mA for 40 min, the gel was stained with Coomassie brilliant blue or was used for the immunoblotting.

Transfer of proteins from the SDS–polyacrylamide gel to a membrane was performed electrophoretically according to the method of Kyhse–Anderson with some modifications using a Semi Dry Electroblotter (Sartorious) for 90 min at 22°C with an electric current of 1 mA/cm^2 slab gel (*16*). As the transfer membrane and buffer, Immobilor Transfer Membrane™ (polyvinylidene difluoride membrane) and 20 mM CAPS buffer (pH 10.5) containing 10% methanol were used, respectively. After the transfer, the membrane was treated with Block Ace™ (4%) for 30 min at 22°C.

The membrane was subjected to immunoreactions. First reaction was performed with the anti-RP S19 rabbit IgG (final concentration 17.4 ng/ml), the anti-RP S19 C-terminal peptide antiserum (30,000-fold dilution) or the anti-C5a antiserum (15,000-fold dilution) in PBS containing 0.03% Tween 20 (PBS/Tween) at 4°C overnight. After washing with 0.3% PBS/Tween, the second reaction was performed with the HRP-conjugated anti-rabbit IgG goat IgG (final concentration 6.7 ng/ml) in 0.03% PBS/Tween for 1 h at 22°C. After washing with 0.3% PBS/Tween, the enhanced chemiluminescence (ECL) reaction was performed on the membrane with ECL Plus Western Blotting Detection System™.

Chemotaxis Assay—Mononuclear cells and neutrophils were at least isolated from heparinized human venous blood of three different healthy donors according to the method of Fernandez *et al*. (*17*) as described previously (*18*). The mononuclear cell fraction contained monocytes at about 20%, and almost all of the cells in the neutrophil

fraction were neutrophils themselves. The mononuclear cells and neutrophils were respectively suspended at a cell density of 1×10^6 cells/ml in RPMI 1,640 containing 10% FBS, and at a cell density of 2×10^6 cells/ml in HBSS containing 0.5% BSA for the multi-well chamber assay.

The multi-well chamber assay was performed according to the method of Falk *et al*. using a Nucleopore filter with a pore size of 5 μm for monocytes and of 3 μm for neutrophils as described previously (*18*, *19*). After incubation for 90 min, each membrane was separated, fixed with methanol and stained with Giemsa solution. The total number of monocytes or of neutrophils migrated beyond the lower surface of the membrane was counted in five microscopic high-power fields. The results are expressed as the number of migrated monocytes or neutrophils.

Measurement of Cytoplasmic Ca^{2+} Concentration Change—Concentration change of cytoplasmic Ca^{2+} was measured by a fluorescent method. In this measurement, monocytes were further enriched using OptiPrep™ according to the instruction manual. The monocyte rich fraction contained monocytes at least 60% when analysed with a fluorescent-activated cell sorter (data not shown). Monocytes at a cell density of 2×10^6 cells/ml in HBSS containing 20 mM HEPES and 3% BSA (pH 7.4) were initially incubated with Fura-2-AM (final concentration of 5 μM) for 30 min at 37°C, and were washed twice with HBSS at room temperature. The Fura-2-loaded monocytes were adjusted their cell density to 2×10^6 cells/ml in HBSS containing 20 mM HEPES and 3% BSA (pH 7.4), and were moved to a cuvette equipped to a fluorescent spectrophotometer (F-2500, Hitachi, Tokyo, Japan). After a couple of minutes, a sample was added to the cuvette, and the fluorescent activities were continuously measured with two excitation wavelengths at 340 and 380 nm and a single emission wavelength at 500 nm at once. The excitation wavelengths at 380 and 340 nm were used to measure the free Fura-2 and the Ca^{2+}-bound Fura-2, respectively. The fluorescent activities of 340 nm/500 nm ($F1$) and of 380 nm/500 nm ($F2$) and the ratio (R) of $F1$ to $F2$ were mechanically given by the spectrophotometer at optional time. The Ca^{2+} concentration (C) was then calculated using the following formula: $C = 224 \times R$, here 224 is the K_d number.

Reverse Passive Arthus Reaction—Guinea pigs were anesthetized with ether, and the medial surface of both hind legs and the flanks were clipped. Reverse passive Arthus reaction was induced as reported previously (*20*). OVA (6.6 mg/ml) in PBS were injected into the left femoral vein of each animal (10 mg OVA/kg). At 5 min later, 10 and 100 μg of anti-OVA rabbit IgG with or without 10^{-7} M C5a/RP S19 chimera in 100 μl of PBS were injected intradermally with 27-gauge needles. Negative and positive control sites received PBS or 10^{-7} M C5a/RP S19 chimera and 10^{-8} M C5a. Before injection of samples, any aggregates were removed by centrifugation at 12,000*g* for 5 min.

Measurement of Plasma Extravasations—Plasma extravasation was measured using the dye-extraction method reported by Udaka *et al*. (*21*) with some modifications (*22*). At 30 min after the injection of samples, 2% Evans blue dye was injected into the right femoral vein of each animal for analysing neutrophil-dependent plasma extravasation. At 11.5 h later, the guinea pigs were killed by exsanguination under ether anesthesia and skin lesions were punched out at 14-mm diameter. The extravasated Evans blue dye in each lesion was extracted in 3 ml formamide for 72 h at 60°C, and the absorbance of the extract was measured at 620 nm using a spectrophotometer (U-2000A, Hitachi). Result was expressed as a ratio of the extravasated dye to that induced by 10^{-8} M C5a using the following formula: the amount of Evans blue dye (μg/site) extravasated by the sample injection/the amount of Evans blue dye extravasated by the 10^{-8} M C5a injection.

Histological Examination—At 12 h later the animals were exsanguinated under ether anesthesia and the skin lesions were immediately resected, then fixed in 10% formalin. Their sections were prepared for the center area of the lesions at 4 μm thickness and stained with haematoxylin and eosin in the usual way. The microscopical pictures were prepared using an automatic microscope, Provis AX (Olympus, Tokyo, Japan), and a digital CCD camera, Penguin 600CL (Pixera, Los Gatos, CA, USA). For the morphometric analysis, we took digital photo pictures of three different areas at least, mainly above the panniculus carnosus muscle, where the leucocyte infiltration is most obvious in the guinea pig skin, at a microscopic high-power field (objective lens ×40) and counted the numbers of infiltrating neutrophils and monocytes as described previously (*6*).

Statistical Analysis—The correlation coefficient was tested by the two-tailed Student's *t*-test. The *P*-values <0.05 were considered to indicate statistical significance ($^*P < 0.05$; $^{**}P < 0.01$).

RESULTS

Preparation of Recombinant C5a and C5a/RP S19 Chimera—The Trx-tag-His-tag-S-tag-C5a bearing the RP S19 C-terminal 12 amino acid residues as well as Trx-tag-His-tag-S-tag-C5a was prepared using an *E. coli* expression system with a trxB-host, Rosseta gami(B) Lys-S. We substituted Cys27 of the human C5a moiety by Arg, and Gly73 of the C5a moiety of the chimeric protein by Asp as described in MATERIALS AND METHODS section. An important part of the plasmid construct and the amino acid sequence of the recombinant proteins are shown in Fig. 1.

These recombinant proteins were purified using HPLC with an affinity column, and the Trx-tag-His-tag was removed with thrombin. The S-tag-C5a and S-Tag-C5a/RP S19 chimera demonstrated single bands in SDS-PAGE as the molecular sizes of 12,500 and 13,900, respectively (Fig. 2A).

In the immunoblotting analysis, the S-tag-chimera was recognized by the anti-C5a antiserum, by the anti-RP S19 rabbit IgG and by the anti-RP S19 C-terminal peptide rabbit antiserum, whereas the S-tag-C5a was recognized only by the anti-C5a antiserum (Fig. 2B). We would respectively use the terms C5a and C5a/RP S19 chimera for the S-tag-C5a and the S-tag-C5a/RP S19 chimera in the following part of this report.

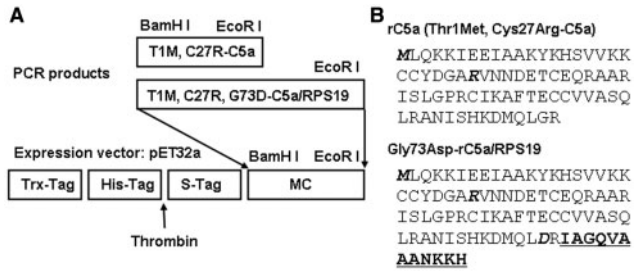

Fig. 1. **Designs of recombinant C5a (Trx-tag-His-tag-S-tag-C5a) and C5a-chimera bearing S19 ribosomal protein (RP S19) C-terminal 12 amino acid residues (Trx-tag-His-tag-S-tag-C5a/RP S19).** (A) Construct of the expression vector, pET32, bearing an artificial C5a cDNA (Thr1Met and Cys27Arg), or its chimeric protein cDNA (Gly73Asp-C5a connected with Ile-Ala-Gly-Gln-Val-Ala-Ala-Ala-Asn-Lys-Lys-His sequence). (B) Amino acid sequences of the product proteins derived from those constructs. The thick italic letters denote the mutated amino acid residues of the recombinant C5a, and the underlined letters denote the RP S19 tail portion connected to the recombinant C5a.

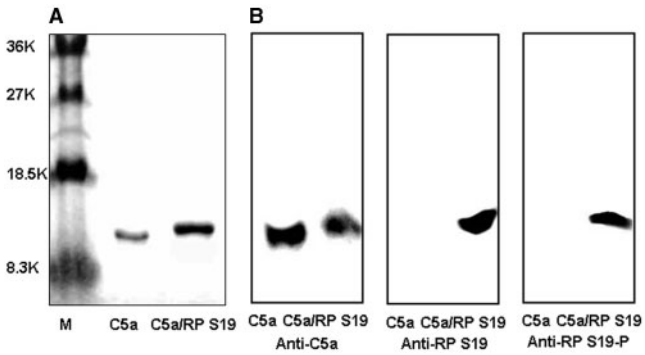

Fig. 2. **Polyacrylamide gel electrophoretical analyses of C5a and C5a/RP S19 chimera.** (A) PAGE in the presence of SDS. The recombinant C5a and the C5a/RP S19 chimera were applied to a 20% polyacrylamide slab gel at an amount of 0.5 μg in 10 μl sample buffer. The protein band in the gel was stained with Coomassie brilliant blue. The numbers at left side denote the molecular weight of marker proteins (M). (B) Immunoblotting analyses. Three sets of C5a and C5a/RP S19 chimera were respectively run in the SDS–PAGE with 20% polyacrylamide slab gels and immunoblotting analyses were performed with an anti-C5a rabbit serum (Anti-C5a), anti-RP S19 rabbit IgG (Anti-S19) or a rabbit antiserum against a synthetic C-terminal peptide of RP S19 (Arg-Lys-Leu-Thr-Pro-Gln-Gly-Gln-Arg-Asp-Leu-Asp-Arg-Ile) (Anti-S19-P), respectively, as the first antibody. The amount of C5a and C5a/RP S19 chimera applied was 0.1 μg/10 μl, 0.2 μg/10 μl or 0.5 μg/10 μl, respectively. After treated with horseradish peroxidase-conjugated anti-rabbit IgG goat IgG, the enhanced chemiluminescence reaction was performed to visualize the antigen band.

Monocyte-Selective Chemoattracting Capacity of C5a/RP S19 Chimera—The chemoattracting capacities of these recombinant proteins to phagocytic leucocytes were examined using the multi-well chamber assay. As shown in Fig. 3, both C5a/RP S19 chimera and C5a attracted monocytes with optimum concentrations at 10^{-7} and 10^{-8} M, respectively. In contrast to this, although C5a attracted neutrophils exhibiting the optimum effect at 10^{-8} M, C5a/RP S19 chimera did not cause the neutrophil chemoattraction.

In the purification, we used identical methods using two affinity column chromatographies (see MATERIALS AND METHODS section) and prepared 5 mg of these recombinant proteins from 500 ml of culture mediums. The different leucocyte chemoattractant patterns between the recombinant proteins neglected a possibility that an *E. coli*-originated protein, which might contaminate in the recombinant protein preparations, attracted these leucocytes. These results also indicated that C5a/RP S19 chimera reproduced the monocyte-selective chemoattraction of the RP S19 dimer.

Prophylactic Inhibition of C5a/RP S19 Chimera-Induced Monocyte Chemotaxis with C5a Receptor Antagonistic/Partial Agonistic Peptide—To confirm whether the C5a/RP S19 chimera-induced monocyte chemoattraction was mediated by the C5a receptor, sensitivity of the monocyte chemotaxis induced by C5a/RP S19 chimera to a prophylactic treatment with an authentic C5a receptor antagonistic/partial agonistic peptide, NMePhe-Lys-Pro-dCha-dCha-dArg, for 15 min at 37°C was examined. As shown in Fig. 4, the C5a/RP S19 chimera-induced monocyte chemotaxis was diminished by pretreatment of indicator monocytes with the C5a receptor antagonistic/partial agonistic peptide in a concentration dependent manner as in the case of C5a-induced chemotaxis. In a statistical analysis at 10^{-6} M for instance of C5a receptor antagonistic/partial agonistic peptide, the monocyte chemotactic potencies of 10^{-9} M C5a and 10^{-8} M C5a/RP S19 chimera were significantly reduced with P-values of <0.0096 and <0.0014, respectively, when compared with the absence of the antagonist peptide.

Cytoplasmic Ca^{2+} Influx of Monocytes Induced by C5a/RP S19 Chimera—A capacity of C5a/RP S19 chimera to induce the cytoplasmic Ca^{2+} influx of monocytes was examined at various concentrations in a comparative manner with C5a. As shown in Fig. 5, C5a and C5a/RP S19 chimera induced the cytoplasmic Ca^{2+} influx with the optimum concentrations at 10^{-8} and 10^{-7} M, respectively. The maximum response induced by C5a/RP S19 chimera was slightly weaker than that induced by C5a.

Antagonistic Effect of C5a/RP S19 Chimera on C5a Receptor of Neutrophils—To examine possible antagonistic effect of C5a/RPS19 chimera on the C5a receptor of neutrophils, we initially observed the alteration of the C5a-induced chemotactic response. We pretreated the indicator neutrophils with C5a/RP S19 chimera at various concentrations, and then observed the chemotactic response of them to C5a. As shown in Fig. 6A, the pretreatment of the neutrophils with C5a/RP S19 chimera prevented the chemotactic response of these cells to C5a in a concentration dependent manner. In contrast to this, the chemotactic response of them to fMLP was not significantly affected by the pretreatment with C5a/RP S19 chimera. In another experiment to examine the competition, we used mixtures of 10^{-9} M C5a and C5a/RP S19 chimera at various concentrations as the chemoattractant. The chemotactic response of neutrophils diminished in association inversely to the increment of C5a/RP S19 chimera concentration (Fig. 6B). At 10^{-8} M of C5a/RP S19 chimera, the 10^{-9} M C5a-induced neutrophil chemoattraction was significantly inhibited ($P < 0.012$).

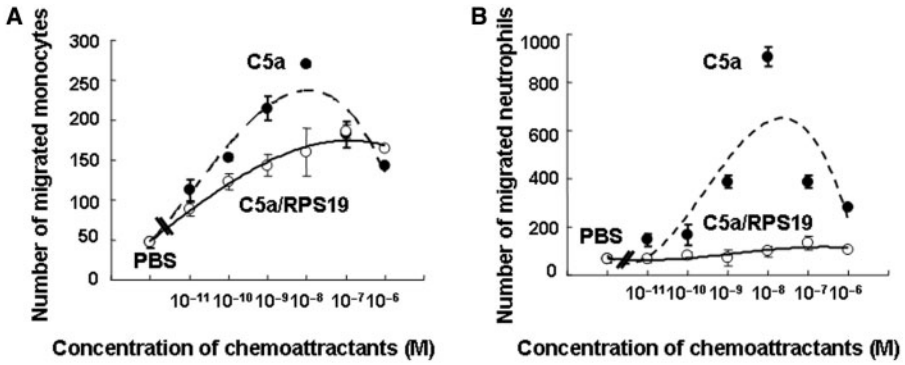

Fig. 3. **Monocyte-predominant chemoattracting capacity of C5a/RP S19 chimera *in vitro*.** The chemotactic capacities of C5a (the broken lines with closed circles) and C5a/RP S19 chimera (the solid lines with open circles) for monocytes and neutrophils were examined. Leucocyte chemotaxis assay utilized was the multi-well chamber assay using a Nucleopore® filter with a pore size of 5 or of 3 μm for monocytes and neutrophils, respectively. After a 90-min incubation, the membrane was stained with Giemsa solution and the total number of monocytes (A) or neutrophils (B) migrated beyond the membrane was counted in five microscopic high-power fields. In the negative control experiment, phosphate-buffered saline containing 0.1 mg/ml bovine serum albumin (PBS) was used as the attractant. The results of a representative examination in at least three different examinations are shown. The experiments were carried out with triplicate samples. Values are expressed as mean ± SD.

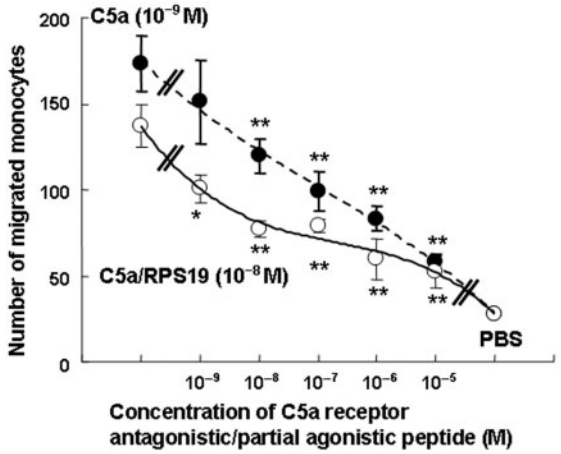

Fig. 4. **Prophylactic inhibition of recombinant protein-induced monocyte chemotaxis with C5a receptor antagonistic/partial agonistic peptide.** The indicator monocytes were pretreated with an authentic C5a receptor antagonistic/partial agonistic peptide, NMePhe-Lys-Pro-dCha-dCha-dArg, at various concentrations for 15 min at 37°C, then used for the chemotaxis assay with C5a (10^{-9} M) or C5a/RP S19 chimera (10^{-8} M). In the negative control experiment, PBS was used as the attractant. The results of a representative examination in at least three different examinations are shown. The experiments were carried out with triplicate samples. Values are expressed as mean ± SD. The *P*-values <0.05 were considered to indicate statistical significance (*$P < 0.05$; **$P < 0.01$).

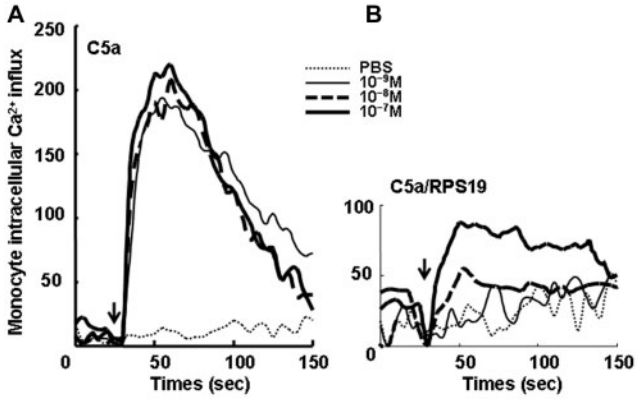

Fig. 5. **Monocyte cytoplasmic Ca^{2+} influx induced by C5a/RP S19 chimera.** (A) In this measurement, monocytes were further enriched using OptiPrep™. The cells (1×10^7 cells/ml) in HBSS containing 20 mM HEPES and 3% BSA (pH 7.4) were initially incubated with calcium-sensitive Fura-2-AM (final concentration of 5 μM) for 30 min at 37°C. The Fura-2-loaded cells (2×10^6 cells/ml) in a cuvette equipped to a fluorescent spectrophotometer (F-2500, Hitachi) were pre-incubated for a couple of minutes, and agitated with a sample directly given into the cuvette, and the fluorescent activities were continuously measured with two excitation wavelengths at 340 and 380 nm and a single emission wavelength at 500 nm at once. The fluorescent activities of 340 nm/500 nm (*F*1) and of 380 nm/500 nm (*F*2) and the ratio (*R*) of *F*1 to *F*2 were mechanically given by the spectrophotometer at optional time. The Ca^{2+} concentration (*C*) was then calculated using the following formula: $C = 224 \times R$, here 224 is the K_d number. The results of a representative examination in at least three different examinations are shown.

We next observed the alteration of the C5a-induced Ca^{2+} influx in neutrophils by the presence of C5a/RP S19 chimera. As shown in Fig. 7A, C5a induced the cytoplasmic Ca^{2+} influx of neutrophils with the optimal concentration at 10^{-8} M. However, neither C5a/RP S19 chimera nor the RP S19 dimer induced the Ca^{2+} influx of neutrophils at any concentrations consistently with the chemoattraction (Fig. 7B and C). In the competitive experiment, the cytoplasmic Ca^{2+} influx induced by 10^{-9} M C5a was diminished by both C5a/RP S19 chimera (Fig. 7D) and RP S19 dimer (Fig. 7E) in a concentration dependent manner.

Induction of Monocyte-Predominant Leucocyte Infiltration with C5a/RP S19 Chimera In Vivo—To confirm the monocyte-predominant chemoattracting capacity of C5a/RP S19 chimera *in vivo*, we histologically examined the leucocyte infiltration pattern at 12 h after

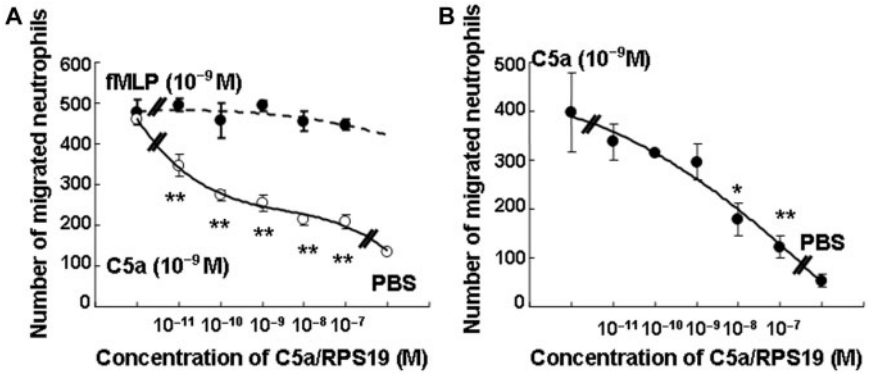

Fig. 6. **Antagonistic effect of C5a/RP S19 chimera on C5a receptor of neutrophils.** (A) The indicator neutrophils were pretreated with C5a/RP S19 chimera at various concentrations for 10 min at 37°C, and used for the chemotaxis assay with 10^{-9} M C5a (the solid line with the open circles) or with 10^{-9} M formyl-Met-Leu-Phe (the broken line with the closed circles). (B) Untreated neutrophils were subjected to the chemotaxis assay with 10^{-9} M C5a in the simultaneous presence of C5a/RP S19 chimera at various concentrations. In the negative control experiment, PBS was used as the attractant. The results of a representative examination in at least three different examinations are shown. The experiments were carried out with triplicate samples. Values are expressed as mean ± SD. The *P*-values <0.05 were considered to indicate statistical significance (**P* < 0.05; ***P* < 0.01).

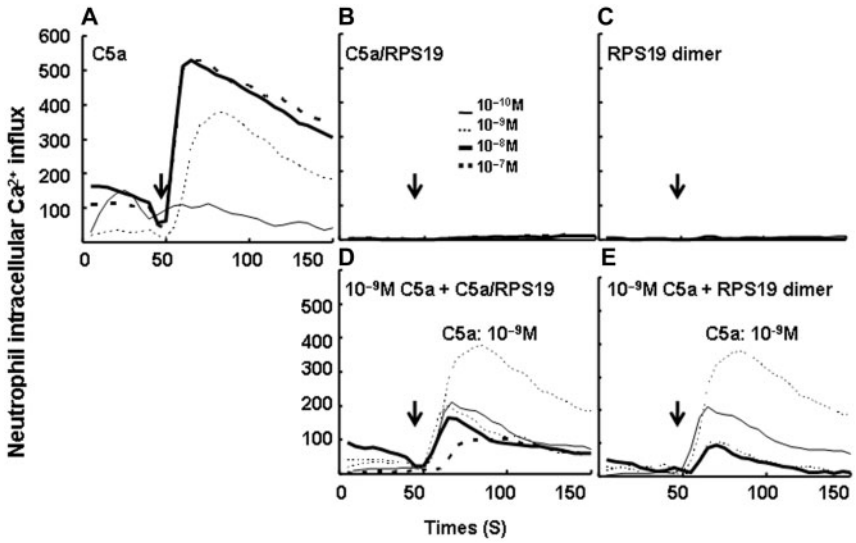

Fig. 7. **Inhibition of C5a-induced neutrophil cytoplasmic Ca^{2+} influx by C5a/RP S19 chimera and RP S19 dimer.** Fura-2-AM-loaded neutrophils (2×10^6 cells/ml) were agitated with C5a (A), C5a/RP S19 chimera (B) or the RP S19 dimer (C) [10^{-10} M (thick solid lines), 10^{-9} M (thick broken lines), 10^{-8} M (thick solid lines) and 10^{-7} M (thin broken lines)], and the change of cytoplasmic Ca^{2+} concentration was recorded in the same way as Fig. 5. Next, the Fura-2-AM-loaded neutrophils were stimulated with 10^{-9} M C5a in the simultaneous presence of C5a/RP S19 chimera (D) or of the RP S19 dimer (E) at various concentrations. The results of a representative examination in at least three different examinations are shown.

injection of 10^{-6} M C5a/RP S19 chimera or C5a into the guinea pig skin. As shown in Fig. 8, C5a/RP S19 chimera induced a monocyte-predominant leucocyte infiltration, whereas C5a induced a mixed-cellular type of infiltration of neutrophils and monocytes.

Inhibition of Neutrophil Infiltration Induced by C5a with Simultaneous Injection of C5a/RP S19 Chimera—Under the assumption that C5a/RP S19 chimera would antagonize the neutrophil infiltration induced by C5a *in vivo*, we histologically examined an alteration of the leucocyte infiltration pattern at 12 h induced with 3×10^{-7} M C5a in the guinea pig skin by simultaneous injection of various concentrations of C5a/RP S19 chimera. Because antibodies recognizing neutrophils or monocytes of the guinea pig in the paraffin section are not available at this moment, we counted neutrophils and monocytes/macrophages on the basis of their morphologies in the haematoxylin and eosin-staining sections. Representative histological pictures and the morphometric analysis data are shown in Fig. 9. At low concentrations such as 3×10^{-8} and 10^{-7} M, C5a/RP S19 chimera inhibited the neutrophil infiltration induced by C5a without augmenting the monocyte infiltration. At higher concentrations such as 3×10^{-7} and 10^{-6} M, C5a/RP S19 chimera augmented the monocyte infiltration in addition to the inhibition of neutrophil infiltration. We then repeated this experiment

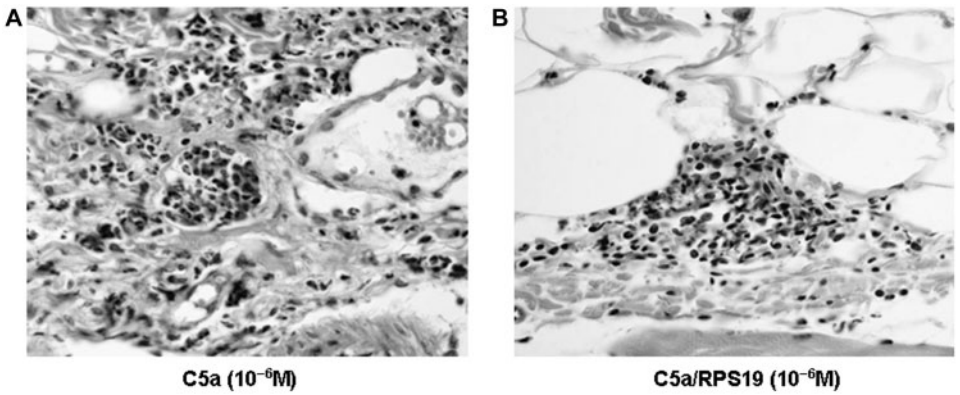

Fig. 8. **Leucocyte infiltration pattern induced by recombinant proteins *in vivo*.** C5a (A) or C5a/RP S19 chimera (B) was intradermally injected with 0.1 ml of 10^{-6} M solution into guinea pigs. At 12 h later, the skin lesions were prepared for usual paraffin sections at 4 μm thickness. Each section was stained with haematoxylin and eosin. Microscopical pictures demonstrated were taken by a digital CCD camera with a 40× objective lens. The results of a representative examination in at least three different examinations are shown.

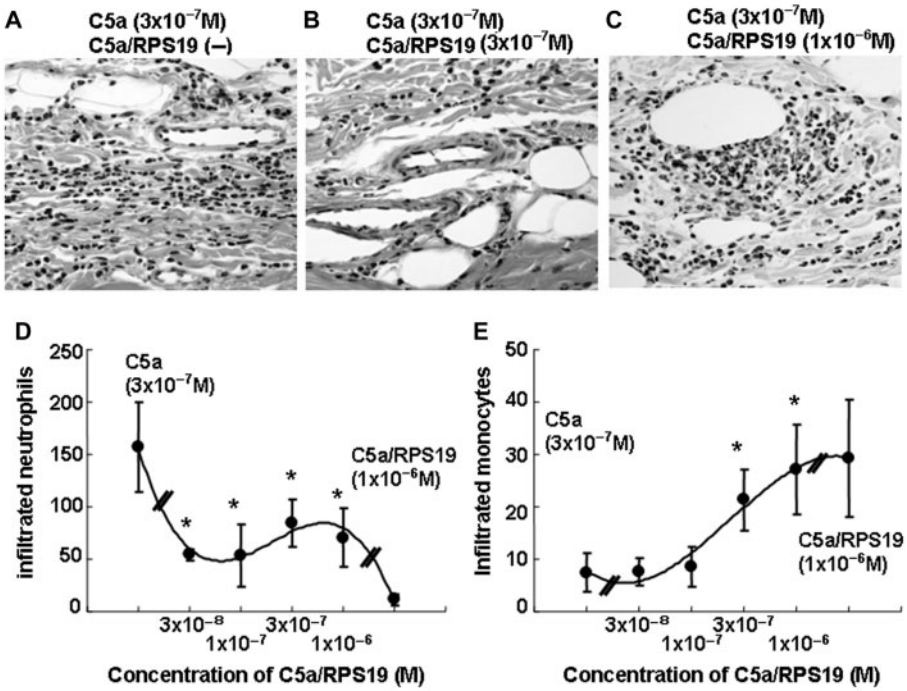

Fig. 9. **Inhibition of C5a-induced neutrophil infiltration by C5a/RP S19 chimera *in vivo*.** C5a (3×10^{-7} M) was intradermally injected in the absence or simultaneous presence of C5a/RPS19 chimera at various concentrations. The skin lesions were resected 12 h later, and their histological specimens and photo pictures were prepared as Fig. 8. Representative pictures of C5a alone (A), and of mixtures with 3×10^{-7} M (B) or with 10^{-6} M C5a/RP S19 chimera (C) are shown. The results of a representative examination in at least two different examinations are shown. In the morphometry, photo pictures of at least three microscopic high-power fields of each histological slide were taken, and the numbers of infiltrated neutrophils (D) and monocytes (E) were counted. Values are expressed as mean leukocyte numbers/high power field ± SD. The *P*-values <0.05 were considered to indicate statistical significance (*$P < 0.05$).

using 10% zymosan-activated guinea pig plasma instead of C5a as the inducer of neutrophil infiltration. The similar results were obtained as in the C5a case (data not shown). These experimental results indicated that C5a/RP S19 chimera behaves as the RP S19 dimer does.

Inhibition of Reverse Passive Arthus Reaction by C5a/RP S19 Chimera—The above results (Figs 6B, 9D and E) suggested that 10^{-7} M of C5a/RP S19 chimera would suppress the neutrophil infiltration without stimulating the monocyte infiltration in some types of acute inflammation in which the complement activation, therefore the C5a generation, is the major mechanism to induce leucocyte infiltration. It is known that the neutrophil predominant infiltration occurs at early phase of Arthus

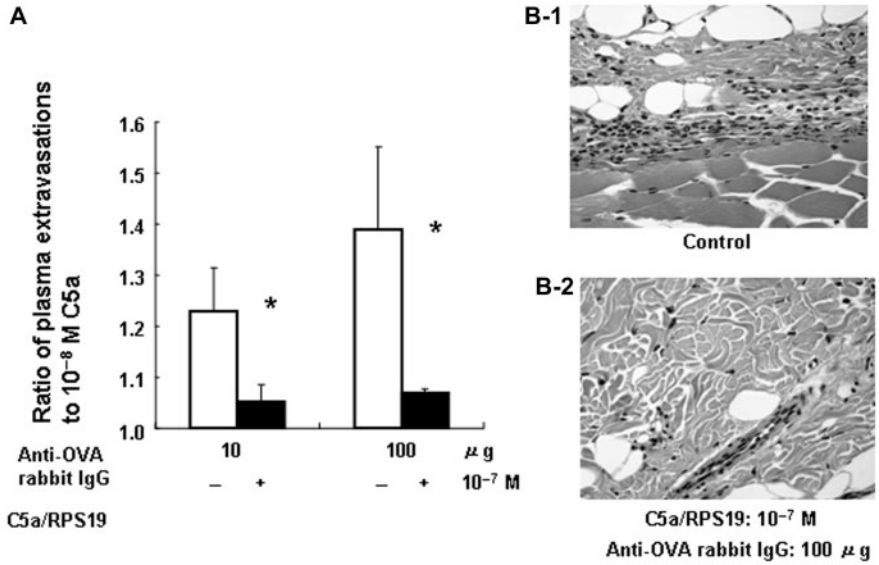

Fig. 10. **Inhibition of neutrophil infiltration associated with plasma extravasation by C5a/RP S19 chimera in reverse passive Arthus reaction in guinea pig skin.** At 5 min after the intravenous injection of the antigen, ovalbumin (OVA), 10 and 100 μg of anti-OVA rabbit IgG in the absence (open columns) or simultaneous presence of 10^{-7} M C5a/RPS19 chimera (closed columns) were intradermally injected. Thirty minutes later, Evans blue dye solution was intravenously given, and the skin lesion was harvested at 11.5 h after the dye injection. After extraction of the dye from the skin lesion, its absorbance was measured at 620 nm (A). Results were expressed as ratio of the plasma extravasation to 10^{-8} M C5a-induced one (see MATERIALS AND METHODS section). For histological examination, the skin lesion was resected at 12 h after the antibody injection, and their histological specimens and photo pictures were prepared as Fig. 8. Injection sites of anti-OVA rabbit IgG with (B-2) or without (B-1) 10^{-7} M C5a/RP S19 chimera are shown. Different four experiments with two set of animals ($n = 8$) were performed and the P-values between the presence and absence of C5a/RP S19 chimera of <0.05 were considered to indicate statistical significance ($^*P < 0.05$).

reaction (type III allergic acute dermatitis), and it is thought that the complement activation is one of the major courses for the neutrophil infiltration in the passive Arthus reaction (*23*). Therefore, we induced a reverse passive Arthus reaction in guinea pigs by administrating an antigen OVA intravenously and its antibodies intradermally as described previously (*20*), and examined the inhibitory effect of C5a/RP S19 chimera on the neutrophil infiltration at 12 h after the phlogistic stimulation. Because the neutrophil infiltration but not the monocyte one accompanies plasma extravasation (*21*, *24*), we quantitatively measured it in addition to the histological observation. To omit the mast cell dependent plasma extravasation at the immediate phase, we intravenously gave Evans blue, which was the indicator dye of plasma extravasation, at 30 min after the intradermal antibody administration (*24*). Consistently to the histologic picture with monocyte-predominant infiltration, the plasma extravasation induced by 10^{-7} M C5a/RP S19 chimera alone (100 μl) was equivalent to that by the negative control PBS (data not shown). To examine the anti-phlogistic potency of C5a/RP S19 chimera, we simultaneously injected 10^{-7} M of it with 10 or 100 μg of anti-OVA rabbit IgG as a mixture intradermally (the volume of each mixture was 100 μl).

The simultaneous presence of 10^{-7} M C5a/RP S19 chimera significantly decreased the amount of extravasated Evans blue dye in the Arthus reaction caused with 10 μg (from 1.23 ± 0.086 to 1.05 ± 0.036 in 10^{-8} M C5a equivalence, $P < 0.030$) and with 100 μg (from 1.39 ± 0.16 to 1.06 ± 0.0080 in 10^{-8} M C5a equivalence, $P < 0.027$) of anti-OVA rabbit IgG (Fig. 10A). Consistently, the neutrophil infiltration histologically observed was obviously reduced by the simultaneous presence of C5a/RP S19 chimera (Fig. 10B). The small number of monocytes/macrophages infiltration was counted in the non-specific esterase-staining sections (*1*). It was not significantly different between the simultaneous stimulation with or without 10^{-7} M C5a/RP S19 chimera as expected (data not shown).

DISCUSSION

To obtain a reagent that effectively antagonized the function of C5a receptor of neutrophils *in vitro* and *in vivo* as the RP S19 dimer does, we have prepared C5a/RP S19 chimera by the new *E. coli* expression system with pET32a vector bearing Trx-tag and with Rosseta gami(B) Lys-S that is a trxB-host *E. coli* strain. We believe that this combination, which have the thioredoxin-promoted disulphide bond formation effect, functioned to form the correct disulphide bridges of C5a/RP S19 chimera as well as the recombinant C5a in the cytoplasm of host *E. coli*.

Using these recombinant proteins, we initially examined whether C5a/RP S19 chimera acted as an agonist and an antagonist of C5a receptor on monocytes and neutrophils, respectively, and induced the monocyte-predominant leucocyte infiltration as the RP S19 dimer does. The results were as good as we had expected. In these experiments, the quantity of monocyte responses as

indicated by migration and cytoplasmic Ca^{2+} influx induced by C5a/PR S19 chimera was weaker than that by C5a (Figs 3A and 5). The difference was small but statistically significant. Similar results were previously observed when we had stimulated monocytes with the RP S19 dimer and C5a to measure the chemotactic response (*6*) and the respiratory burst reaction (*7*). For instance, the respiratory burst reaction of monocytes to C5a and to the RP S19 dimer was 3.4×10^{-7} and 2.1×10^{-7} unit/cell, respectively (*7*). We do not know the mechanism to induce the different quantity of monocyte response between C5a and C5a/PR S19 chimera or the RP S19 dimer at this moment. However, the difference between C5a and C5a/PR S19 chimera is that the latter has the C-terminal region of RP S19 and the receptor-binding β-carboxyl group instead of the α-carboxyl group of the former, and the commonness between C5a/PR S19 chimera and the RP S19 dimer is to bear the C-terminal region of RP S19 and the receptor-binding β-carboxyl group. As a rational consequence of them, we could speculate that either of the C-terminal regions of RP S19 or the receptor-binding β-carboxyl group would be reducing efficacy of the ligand-receptor interaction.

We then used C5a/RP S19 chimera to alter the C5a-induced leucocyte infiltration pattern *in vivo*. C5a/RP S19 chimera effectively inhibited the C5a-induced neutrophil infiltration even at relatively low concentrations. In contrast to this, C5a/RP S19 chimera needs a higher concentration to augment the monocyte infiltration. This may be a reflection of the difference in the total number of the C5a receptor per cell between these cell types, 150,000–200,000 on a neutrophil and 80,000–100,000 on a monocyte (*25*).

These experimental results *in vivo* and the interpretation for them raised an idea that the low dose such as 10^{-7} M of C5a/PR S19 chimera would be useful to selectively prevent neutrophil infiltration without augmenting the monocyte infiltration in the acute inflammation. Meeting our expectation, the low dose C5a/PR S19 chimera suppressed the neutrophil infiltration including the neutrophil-dependent permeability enhancement in an experimental allergic acute dermatitis, reverse passive Arthus reaction. Different from the infectious inflammation, the inflammatory response in allergic or autoimmune diseases is solely pernicious. To block the neutrophil infiltration at acute phase of the harmful inflammation must be most beneficial for patients. We hope that this report would help to develop a therapeutic method blocking such pernicious neutrophil infiltration.

Recently, widespread expression of the C5a receptor in non-myeloid cells such as hepatocytes, lung vascular smooth muscle cells, bronchial and alveolar epithelial cells, articular chondrocytes and astrocytes, has been reported (*26–28*). At present time no one knows the presence or absence of functional subtypes in the non-myeloid cell C5a receptor. The set of recombinant C5a and C5a/RP S19 chimera would be useful to study the functional subtype of C5a receptor, whether neutrophil-type or monocyte-type. C5a/RP S19 chimera should also facilitate the elucidation of the mechanism that underlies the differences between the monocyte-type and neutrophil-type C5a receptor responses in these cell species.

We have recently reported that mouse fibroblast-derived NIH3T3 cells, which do not constantly activate the C5a receptor gene, began to express it during apoptotic process. The rate of apoptotic process of these cells was retarded and accelerated by the presence of C5a and the RP S19 dimer, respectively (*13*). C5a/RP S19 chimera must be also a good tool to examine whether this phenomenon is common and to elucidate which signal transduction pathway involves in the augmentation of apoptosis.

The authors are grateful to Miss T. Kubo and Miss T. Matsuda of Faculty of Medical and Pharmaceutical Sciences, Kumamoto University for technical assistance. We also thank Dr Peter Monk of University Sheffield, UK for invaluable advice on English usage in this report.

REFERENCES

1. Nishiura, H., Shibuya, Y., Matsubara, S., Tanase, S., Kambara, T., and Yamamoto, T. (1996) Monocyte chemotactic factor in rheumatoid arthritis synovial tissue: probably a cross-linked derivative of S19 ribosomal protein. *J. Biol. Chem.* **271**, 878–882
2. Shi, L., Tsurusaki, S., Futa, N., Sakamoto, T., Matsuda, T., Nishino, N., Kunitomo, R., Kawasuji, M., Tokita, K., and Yamamoto, T. (2005) Monocyte chemotactic S19 ribosomal protein dimer in atherosclerotic vascular lesion. *Virchows Arch.* **447**, 747–755
3. Nishiura, H., Tanase, S., Shibuya, Y., Nishimura, T., and Yamamoto, T. (1999) Determination of the cross-linked residues in homo-dimerization of S19 ribosomal protein concomitant with exhibition of monocyte chemotactic activity. *Lab. Invest.* **79**, 915–923
4. Horino, K., Nishiura, H., Ohsako, T., Shibuya, Y., Hiraoka, T., Kitamura, N., and Yamamoto, T. (1998) A monocyte chemotactic factor, S19 ribosomal protein dimer, in phagocytic clearance of apoptotic cells. *Lab. Invest.* **78**, 603–617
5. Nishimura, T., Horino, K., Nishiura, H., Shibuya, Y., Hiraoka, T., Tanase, S., and Yamamoto, T. (2001) Apoptotic cells of an epithelial cell line, AsPC-1, release monocyte chemotactic S19 ribosomal protein dimer. *J. Biochem.* **129**, 445–454
6. Nishiura, H., Shibuya, Y., and Yamamoto, T. (1998) S19 ribosomal protein cross-linked dimer causes monocyte-predominant infiltration by means of molecular mimicry to complement C5a. *Lab. Invest.* **78**, 1615–1623
7. Revollo, I., Nishiura, H., Shibuya, Y., Oda, Y., Nishino, N., and Yamamoto, T. (2005) Agonist and antagonist dual effect of the cross-linked ribosomal protein dimer in the C5a receptor-mediated respiratory burst reaction of phagocytic leukocytes. *Inflam. Res.* **54**, 82–90
8. Shibuya, Y., Shiokawa, M., Nishiura, H., Nishimura, T., Nishino, N., Okabe, H., Takagi, K., and Yamamoto, T. (2001) Identification of receptor binding sites of monocyte chemotactic S19 ribosomal protein dimer. *Am. J. Pathol.* **159**, 2293–2301
9. Shrestha, A., Shiokawa, M., Nishimura, T., Nishiura, H., Tanaka, Y., Nishino, N., Shibuya, Y., and Yamamoto, T. (2003) Switch moiety in agonist/antagonist dual effect of S19 ribosomal protein dimer on leukocyte chemotactic C5a receptor. *Am. J. Pathol.* **162**, 1381–1388
10. Bao, L., Gerard, N.P., Eddy, R.L. Jr., Shows, T.B., and Gerard, C. (1992) Mapping of genes for the human C5a receptor (C5AR), human FMLP receptor (FPR), and two FMLP receptor homologue orphan receptors (FPRH1, FPRH2) to chromosome 19. *Genomics* **13**, 437–440
11. Umeda, Y., Shibuya, Y., Semba, U., Tokita, K., Nishino, N., and Yamamoto, T. (2004) Guinea pig ribosomal protein as

precursor of C5a receptor-directed monocyte-selected leukocyte chemotactic factor. *Inflam. Res.* **53**, 623–630
12. Konteatis, Z.D., Siciliano, S.J., Van-Riper, G., Molineaux, C.J., Pandya, S., Fischer, P., Rosen, H., Mumford, R.A., and Springer, M.S. (1994) Development of C5a receptor antagonists: Differential loss of functional responses. *J. Immunol.* **153**, 4200–4205
13. Nishiura, Y., Tanase, S., Shibuya, Y., Futa, N., Sakamoto, T., Higginbottom, A., Monk, P., Zwirner, J., and Yamamoto, T. (2005) S19 ribosomal protein dimer augments metal-induced apoptosis in a mouse fibroblastic cell line by ligation of the C5a receptor. *J. Cell. Biochem.* **94**, 540–553
14. Paczkowski, N.J., Finch, A.M., Whitmore, J.B., Shot, A.J., Wong, A.K., Monk, P.N., Cain, S.A., Fairlie, D.P., and Taylor, S.M. (1999) Pharmacological characterization of antagonists of the C5a receptor. *Br. J. Pharm.* **128**, 1461–1466
15. Laemmli, U.K. (1970) Cleavage of structural proteins during the assembly of the head of bacteriophage T4. *Nature* **227**, 680–685
16. Kyhse-Andersen, J. (1984) Electroblotting of multiple gels: a simple apparatus without buffer tank for rapid transfer of proteins from polyacrylamide to nitrocellulose. *J. Biochem. Biophys. Methods* **10**, 203–209
17. Fernandez, H.N., Henson, P.M., Otani, A., and Hugli, T.E. (1978) Primary structural analysis of the polypeptide portion of human C5a anaphylatoxin: polypeptide sequence determination and assignment of the oligosaccharide attachment site in C5a. *J. Immunol.* **120**, 109–117
18. Matsubara, S., Yamamoto, T., Tsuruta, T., Takagi, K., and Kambara, T. (1991) Complement C4-derived monocyte-directed chemotaxis-inhibitory factor: a molecular mechanism to cause polymorphonuclear leukocyte-predominant infiltration in rheumatoid arthritis synovial cavities. *Am. J. Pathol.* **138**, 1279–1291
19. Falk, W., Goldwin, R.H., and Leonard, E.J. (1980) A 48 well micro-chemotaxis assembly for rapid and accurate measurement of leukocyte migration. *J. Immunol. Method* **33**, 239–247
20. Szalai, A.J., Digerness, S.B., Agrawal, A., Kearney, J.F., Bucy, R.P., Niwas, S., Kilpatrick, J.M., Babu, Y.S., and Volanakis, JE. (2000) The Arthus reaction in rodents: species-specific requirement of complement. *J. Immunol.* **164**, 463–468
21. Udaka, K., Takeuchi, Y., and Movat, H.Z. (1970) Simple method for quantitation of enhanced vascular permeability. *Proc. Soc. Exp. Biol. Med.* **133**, 1384–1387
22. Tokita, K. and Yamamoto, T. (2004) Differential role of neutrophils and monocytes during subcutaneous plasma extravasation. *Lab. Invest.* **84**, 1174–1184
23. Cochrane, C.G. and Janoff, A. (1974) The Arthus reaction: a model of neutrophil and complement-mediated injury in *The Inflammatory Process* (Zweifach, B.W., Grant, L., and McCluskey, R.T., eds.) Chapter 3, Vol. 3, 2nd edn, Academic Press, New York.
24. Tokita, K., Uchida, Y., and Yamamoto, T. (2006) Roles of leukocytosis and cysteinyl leukotriene in polymorphonuclear leukocyte-dependent plasma extravasation. *J. Leukoc. Biol.* **80**, 1308–1319
25. Chenoweth, D.E., Goodman, M.G., and Weigle, W.O. (1982) Demonstration of a specific receptor for human C5a anaphylatoxin on murine macrophages. *J. Exp. Med.* **156**, 912–917
26. Haviland, D.L., McCoy, R.L., Whitehead, W.T., Akama, H., Molmenti, E.P., and Brown, A. (1995) Cellular expression of the C5a anaphylatoxin receptor (C5aR): demonstration of C5aR on nonmyeloid cells of the liver and lung. *J. Immunol.* **154**, 1861–1869
27. Onuma, H., Masuko-Hongo, K., Yuan, G., Sakata, M., Nakamura, H., and Kato, T. (2002) Expression of the anaphylatoxin receptor C5aR (CD88) by human articular chondrocytes. *Rheumatol. Int.* **22**, 52–55
28. Gasque, P., Chan, P., Fontaine, M., Ischenko, A., Lamacz, M., and Gotze, O. (1995) Identification and characterization of the complement C5a anaphylatoxin receptor on human astrocytes. *J. Immunol.* **155**, 4882–4889